

# Minimum Area All-flush Triangles Circumscribing a Convex Polygon\*

Kai Jin<sup>1</sup> and Zhiyi Huang<sup>2</sup>

<sup>1</sup> Department of Computer Science, University of Hong Kong  
cscjkk@gmail.com

<sup>1</sup> Department of Computer Science, University of Hong Kong  
hzhyyi.tcs@gmail.com

---

## Abstract

In this paper, we consider the problem of computing the minimum area triangle that circumscribes a given  $n$ -sided convex polygon touching edge-to-edge. In other words, we compute the minimum area triangle that is the intersection of 3 half-planes out of  $n$  half-planes defined by a given convex polygon. Previously,  $O(n \log n)$  time algorithms were known which are based on the technique for computing the minimum weight  $k$ -link path given in [2, 12]. By applying the new technique proposed in Jin's recent work for the dual problem of computing the maximum area triangle inside a convex polygon, we solve the problem at hand in  $O(n)$  time, thus justify Jin's claim that his technique may find applications in other polygonal inclusion problems. Our algorithm actually computes all the local minimal area circumscribing triangles touching edge-to-edge.

**1998 ACM Subject Classification** I.3.5 Computational Geometry and Object Modeling

**Keywords and phrases** Geometric optimization, Polygonal inclusion problem, Triangle, Convex polygon, Algorithm

**Digital Object Identifier** 10.4230/LIPIcs..2016.23

## 1 Introduction

Computing the *Maximum Area Triangle* (MAT) inside a given convex polygon  $P$  is perhaps the most classic polygonal inclusion problem and draws some attention recently. The linear time algorithm proposed 38 years ago by Dobkin and Snyder [5] was found incorrect by V. Keikha et. al. [8] in this year. Later, the first author of this paper designed a linear time algorithm for this problem by using a new technique so called "Rotate-and-Kill" (see [7]). Briefly speaking, it enumerates a vertex pair  $(V, V')$  of  $P$  and maintain the vertex  $V''$  with the furthest distance to the line defined by  $V$  and  $V'$ . Let  $V + 1$  denote the clockwise next vertex of  $V$ . At each iteration of the algorithm, it determines in constant time that either no pair in  $\{(V, V' + 1), (V, V' + 2), \dots\}$  can form an edge of any MAT and thus kills  $V$ , i.e., moves on to  $(V + 1, V')$ , or no pair in  $\{(V + 1, V'), (V + 2, V'), \dots\}$  can form an edge of any MAT and thus kills  $V'$ , i.e., moves on to  $(V, V' + 1)$ . This algorithm and its analysis are simpler than a previous known linear time algorithm given by Chandran and Mount [4].

In this paper, we consider a dual polygonal inclusion problem: computing the minimum area triangle that circumscribes  $P$  touching edge-to-edge, namely, computing the *Minimum area All-Flush Triangle* (MFT) circumscribes  $P$ . Previously, this dual problem was discussed as applications of techniques for computing the minimum weight  $k$ -link path in [2, 12].

---

\* This work was partially supported by someone.



© Kai Jin, Zhiyi Huang;  
licensed under Creative Commons License CC-BY

Editors: John Q. Open and Joan R. Acces; Article No. 23; pp. 23:1–23:15



Leibniz International Proceedings in Informatics

LIPICS Schloss Dagstuhl – Leibniz-Zentrum für Informatik, Dagstuhl Publishing, Germany

However, to the best of our knowledge, only  $O(n \log n)$  time algorithms can be obtained by using their techniques, where  $n$  is the number of edges of  $P$ . By applying the Rotate-and-Kill technique, we present the first  $O(n)$  time algorithm for solving the MFT problem.

As the new technique is applicable in solving both the MAT and MFT problems, it may be worth to examine whether other polygonal inclusion problems (e.g. the maximum 4-gon problem considered in [3]) admit more efficient solutions based on this technique.

**Related work.** Chandran and Mount's algorithm [4] computes all the minimum area triangle enclosing  $P$  and MAT in  $P$  simultaneously, and is an extension of O'Rourke et. al.'s linear time algorithm [11] for computing the minimum area triangle enclosing  $P$ . The latter is an improvement over an  $O(n \log^2 n)$  time algorithm given by Klee and Laskowski [9]. Jin's algorithm is also extendable to compute these two extremal triangles simultaneously as shown in [7]. Moreover, [1] and [10] considered the minimum area/perimeter circumscribing  $k$ -gons. We refer the readers to the introduction of [6] and [7] for more related work.

**Note.** Although the MFT and MAT problems are often viewed as dual to each other (as claimed in [2, 12]), they are only dual from the combinatorial perspective. There is no evidence that an instance of the MFT problem can be reduced to (whether in linear time or not) an instance of the MAT problem. We will shortly discuss it in appendix B.

## 1.1 Notations

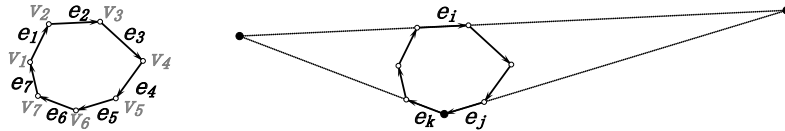
Let  $v_1, \dots, v_n$  be a clockwise enumeration of the vertices of the given convex polygon  $P$ . Assume that no three vertices lie in the same line. Let  $e_1, \dots, e_n$  denote the  $n$  edges of  $P$ , where  $e_i$  is the directed line segment  $\overrightarrow{v_i v_{i+1}}$ . For ease of discussion, assume all edges of  $P$  are **pairwise-nonparallel**. Let  $\partial P$  denote  $P$ 's boundary.

Let  $a+1, a-1$  denote the clockwise next and previous edge of edge  $a$  respectively.

For each edge  $e_i$ , denote by  $\ell_i$  the extended line of  $e_i$ , and  $h_i$  the half-plane delimited by  $\ell_i$  and containing  $P$ . For three distinct edges  $e_i, e_j, e_k$  such that  $e_i, e_j, e_k$  lie in clockwise order, denote by  $\Delta e_i e_j e_k$  the region bounded by  $h_i, h_j, h_k$ , and denote its area by  $\text{Area}(\Delta e_i e_j e_k)$ . (Note that whenever we write  $\Delta e_i e_j e_k$ , we assume that  $e_i, e_j, e_k$  lie in clockwise order.)

**Chasing relation between edges.** Given two distinct edges  $e_i, e_j$ , we say that  $e_i$  is *chasing*  $e_j$ , denoted by  $e_i \prec e_j$ , if  $v_j$  is closer to the extended line of  $e_i$  than  $v_{j+1}$ ; equivalently, if  $v_{i+1}$  is closer to the extended line of  $e_j$  than  $v_i$ . By the pairwise-nonparallel assumption of edges, for any pair of edges, exactly one of them is chasing the other. For example, in Figure 1,  $e_1$  is chasing  $e_2$  and  $e_3$ , whereas  $e_4, e_5, e_6, e_7$  are chasing  $e_1$ .

**All-flush circumscribing triangles.** Assume  $e_i, e_j, e_k$  are distinct edges of  $P$  lying in clockwise order. When  $e_i \prec e_j, e_j \prec e_k$  and  $e_k \prec e_i$ , region  $\Delta e_i e_j e_k$  is indeed a triangle that circumscribes  $P$ , and it is called an *all-flush circumscribing triangle*, or *all-flush triangle* for short. Otherwise,  $\Delta e_i e_j e_k$  is unbounded and  $\text{Area}(\Delta e_i e_j e_k)$  is infinity.



■ **Figure 1** Illustration of the chasing relation and all-flush circumscribing triangles.

**3-stable.** Consider any all-flush triangle  $\triangle e_i e_j e_k$ . Edge  $e_i$  is considered *stable* in this triangle if  $\text{Area}(\triangle e_i e_j e_k) \leq \text{Area}(\triangle e_{i'} e_j e_k)$  for any  $e_{i'}$ ; edge  $e_j$  is considered *stable* in this triangle if  $\text{Area}(\triangle e_i e_j e_k) \leq \text{Area}(\triangle e_i e_j e_{k'})$  for any  $e_{k'}$ ; and  $e_k$  is considered *stable* if  $\text{Area}(\triangle e_i e_j e_k) \leq \text{Area}(\triangle e_i e_j e_{k'})$  for any  $e_{k'}$ .  $\triangle e_i e_j e_k$  is *3-stable* if  $e_i, e_j, e_k$  are stable.

## 1.2 Technique overview

In our algorithm, we compute all 3-stable triangles. Then, by selecting the minimum among them, we compute the minimum area all-flush triangle that circumscribes  $P$ .

We first establish that any two 3-stable triangles are interleaving (see Definition 1 and Lemma 2), and compute one 3-stable triangle by a trivial algorithm (see Section 2). Denote the result 3-stable triangle by  $\triangle e_r e_s e_t$ . By Lemma 2, any 3-stable triangle interleaves  $\triangle e_r e_s e_t$ , and hence has two edges  $b, c$  such that  $b \in \{e_s, \dots, e_t\}$  whereas  $c \in \{e_t, \dots, e_r\}$ . We then compute all 3-stable triangles in the following **Rotate-and-Kill** process.

Initially, we set two pointers  $(b, c) = (e_s, e_t)$ . In each iteration, we first compute an edge  $a = \text{OPT}_{b,c}$ , where  $\text{OPT}_{b,c}$  is defined to be the edge  $e_i$  so that  $\text{Area}(\triangle e_i b c)$  is minimum. (See a rigorous definition in Definition 3.) The computation of  $a$  only costs amortized  $O(1)$  time due to a monotonicity of  $\text{OPT}_{b,c}$  stated in Lemma 5 and due to the fact that pointers  $b, c$  move in clockwise during the process. Next, check whether  $\triangle abc$  is 3-stable and report it if so. We then go to the next iteration by either killing  $b$  (i.e. moving pointer  $b$  to its next edge) or killing  $c$  (i.e. moving pointer  $c$  to its next edge). We say that edge pair  $(e_j, e_k)$  is **dead** if there does not exist an edge  $e_i$  such that  $\triangle e_i e_j e_k$  is 3-stable. We make sure that  $b$  is killed only when all pairs in  $\{(b, c+1), (b, c+2), \dots, (b, e_r)\}$  are dead, and  $c$  is killed only when all pairs in  $\{(b+1, c), (b+2, c), \dots, (e_t, c)\}$  are dead, thus our algorithm will not miss any 3-stable triangles. Eventually,  $(b, c)$  reaches  $(e_t, e_r)$  and we terminate the Rotate-and-Kill process.

The entire process runs in linear time because the **decision-condition** we applied for killing  $b$  or  $c$  is amazingly simple and can be computed in amortized  $O(1)$  time, and we note that the key of our approach lies in designing this condition. Be aware that in each iteration, either  $\{(b, c+1), (b, c+2), \dots, (b, e_r)\}$  are all dead, or  $\{(b+1, c), (b+2, c), \dots, (e_t, c)\}$  are all dead. Otherwise, there exist two 3-stable triangles  $\triangle abc'$  and  $\triangle a'b'c$  which are not interleaving, which contradicts Lemma 2. Therefore, it is possible to find such a decision-condition.

## 1.3 A preliminary lemma

Given two points  $X, X'$  on  $\partial P$ . If we travel along  $\partial P$  in clockwise from  $X$  to  $X'$ , we will pass through a boundary-portion of  $P$ ; the endpoints-inclusive and endpoints-exclusive versions of this portion are denoted by  $[X \circ X']$  and  $(X \circ X')$  respectively.

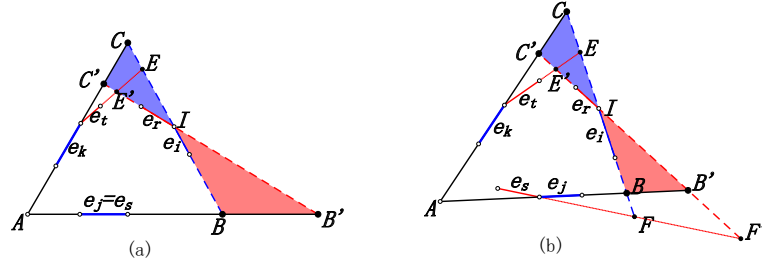
► **Definition 1.** We say that two 3-stable triangles  $\triangle e_i e_j e_k$  and  $\triangle e_r e_s e_t$  are *interleaving* if

1. one edge in  $\{e_r, e_s, e_t\}$  lies in  $\{e_i, e_{i+1}, \dots, e_j\}$ , and another lies in  $\{e_j, e_{j+1}, \dots, e_k\}$ , and another lies in  $\{e_k, e_{k+1}, \dots, e_i\}$ ; and
2. one edge in  $\{e_i, e_j, e_k\}$  lies in  $\{e_r, e_{r+1}, \dots, e_s\}$ , and another lies in  $\{e_s, e_{s+1}, \dots, e_t\}$ , and another lies in  $\{e_t, e_{t+1}, \dots, e_r\}$ .

In other words, we can find a list of edges  $e_{a_1}, \dots, e_{a_6}$  which lie in clockwise order (here, neighbors may be identical), so that  $\{e_{a_1}, e_{a_3}, e_{a_5}\} = \{e_i, e_j, e_k\}$  and  $\{e_{a_2}, e_{a_4}, e_{a_6}\} = \{e_r, e_s, e_t\}$ .

► **Lemma 2.** Any two 3-stable triangles are interleaving.

**Proof.** Suppose that  $\triangle e_i e_j e_k, \triangle e_r e_s e_t$  are two 3-stable triangles which are not interleaving. There can be two cases: (1) they share one common edge; and (2) they share no common edge.



■ **Figure 2** If two triangles are not interleaving, they cannot be both 3-stable.

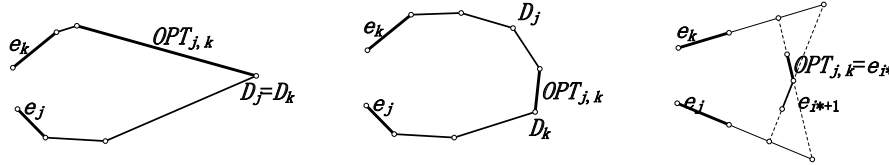
First, let us consider case (1). Without loss of generality, assume  $e_j = e_s$ . Further assume that  $e_t, e_r$  lie in  $(v_{k+1} \circ v_i)$ , as shown in Figure 2 (a). Otherwise,  $e_k, e_i$  lie in  $(v_{t+1} \circ v_r)$  and it is symmetric. Let  $I$  be the intersection of  $\ell_i$  and  $\ell_r$ . Let  $B, C, E, B', C', E'$  be the intersections as shown in the figure. Since  $e_i$  is stable in  $\triangle e_i e_j e_k$ , we get  $\text{Area}(e_i e_j e_k) \leq \text{Area}(e_r e_j e_k)$ . Equivalently,  $\text{Area}(\triangle ICC') \leq \text{Area}(\triangle IBB')$ . This implies  $\text{Area}(\triangle IEE') < \text{Area}(\triangle IBB')$ . Equivalently,  $\text{Area}(\triangle e_i e_s e_t) < \text{Area}(\triangle e_r e_s e_t)$ , which implies that  $e_r$  is not stable in  $\triangle e_r e_s e_t$ . The proof for case (2) is similar and is illustrated in Figure 2 (b). ◀

## 2 Compute one 3-stable triangle

In this section we compute one 3-stable triangle  $\triangle abc$  ( $a, b, c$  denote three edges of  $P$ ).

For each edge  $e_i$ , let  $D_i$  denote the vertex with the furthest distance to  $\ell_i$ .

► **Definition 3.** For any edge pair  $(e_j, e_k)$  such that  $e_j \prec e_k$ , we define an edge  $\text{OPT}_{j,k}$  as follows. If  $D_j = D_k = v_x$ , we define  $\text{OPT}_{j,k}$  to be  $e_{x-1}$ . Otherwise, we define  $\text{OPT}_{j,k}$  to be the smallest  $i^*$  such that  $\text{Area}(\triangle e_{i^*} e_j e_k) = \min(\text{Area}(\triangle e_i e_j e_k) \mid e_i \in \{e_{k+1}, \dots, e_{j-1}\})$ .



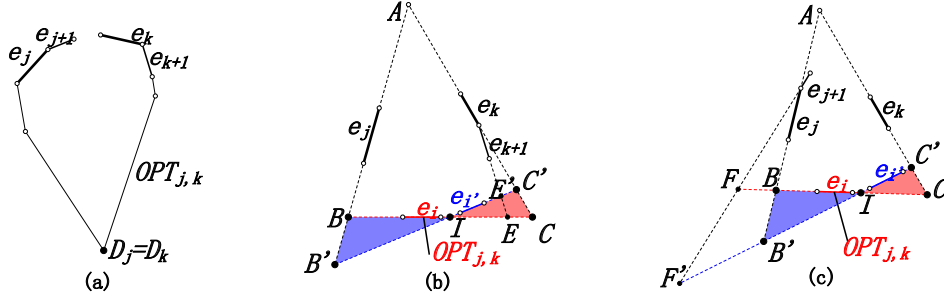
■ **Figure 3** Illustration of the definition of  $\text{OPT}_{j,k}$ .

► **Lemma 4** (Unimodality of  $\text{Area}(\triangle e_i e_j e_k)$  for fixed  $j, k$ ). Assume  $e_j \prec e_k$  and  $D_j \neq D_k$ . We claim that  $\{\text{Area}(\triangle e_i e_j e_k) \mid e_i \in (D_j \circ D_k)\}$  is unimodal. More specifically,  $\text{Area}(\triangle e_i e_j e_k)$  strictly decreases when  $e_i$  is enumerated in clockwise from the next edge of  $D_j$  to  $\text{OPT}_{j,k}$ ; and strictly increases from the **next edge of**  $\text{OPT}_{j,k}$  to the previous edge of  $D_k$ ; moreover,  $\text{Area}(\triangle e_{i^*+1} e_j e_k) \geq \text{Area}(\triangle e_{i^*} e_j e_k)$  for  $e_{i^*} = \text{OPT}_{j,k}$  and sometimes this equality holds (as shown in the last picture of Figure 3). As a corollary, when  $e_i$  is stable in some all-flush triangle  $\triangle e_i e_j e_k$ , we can infer that  $e_i = \text{OPT}_{j,k}$  or  $e_i$  is the next edge of  $\text{OPT}_{j,k}$ .

The trivial proof of the above lemma is omitted.

► **Lemma 5** (Bi-monotonicity of  $\{\text{OPT}_{j,k} \mid e_j \prec e_k\}$ ).

1. Assume  $e_j \prec e_k$  and  $e_j \prec e_{k+1}$ . We claim that either  $\text{OPT}_{j,k} = \text{OPT}_{j,k+1}$ , or these two edges  $\text{OPT}_{j,k}, \text{OPT}_{j,k+1}$  lie in clockwise order in the edge interval  $[e_{k+1}, \dots, e_{j-1}]$ .



■ **Figure 4** Proof of the bi-monotonicity of  $\{\text{OPT}_{j,k}\}$ .

2. Assume  $e_j \prec e_k$  and  $e_{j+1} \prec e_k$ . We claim that either  $\text{OPT}_{j,k} = \text{OPT}_{j+1,k}$ , or these two edges  $\text{OPT}_{j,k}, \text{OPT}_{j+1,k}$  lie in clockwise order in the edge interval  $[e_{k+1}, \dots, e_j]$ .

**Proof.** 1. First, consider the case where  $D_j = D_k$ , as shown in Figure 4 (a). If  $D_{k+1} = D_j$ , we have  $\text{OPT}_{j,k+1} = \text{OPT}_{j,k}$ , otherwise  $\text{OPT}_{j,k+1}$  must be an edge that lies in  $(D_j \cap D_{k+1})$ , which implies that  $\text{OPT}_{j,k}, \text{OPT}_{j,k+1}$  lie in clockwise order in the edge interval  $[e_{k+1}, \dots, e_j]$ . Then, consider the case  $D_j \neq D_k$ . Assume  $\text{OPT}_{j,k} = e_i$ , as shown in Figure 4 (b). Assume  $e_{i'}$  is an arbitrary edge in  $(D_j \cap v_i)$ . We shall prove that  $\text{OPT}_{j,k+1} \neq e_{i'}$ . Assume  $\ell_i$  intersects  $\ell_j, \ell_k, \ell_{k+1}$  at  $B, C, E$  respectively, and  $\ell_{i'}$  intersects  $\ell_j, \ell_k, \ell_{k+1}$  at  $B', C', E'$  respectively. Let  $I$  denote the intersection of  $\ell_i$  and  $\ell_{i'}$ . According to the definition of  $\text{OPT}_{j,k}$ , we have  $\text{Area}(\triangle e_i e_j e_k) < \text{Area}(\triangle e_{i'} e_j e_k)$ . Equivalently,  $\text{Area}(\triangle ICC') < \text{Area}(\triangle IBB')$ . This implies  $\text{Area}(\triangle IEE') < \text{Area}(\triangle IBB')$ . Equivalently,  $\text{Area}(\triangle e_i e_j e_{k+1}) < \text{Area}(\triangle e_{i'} e_j e_{k+1})$ . This means  $\text{OPT}_{j,k+1} \neq e_{i'}$ . The proof of Claim 2 is similar and omitted; see Figure 4 (c). ◀

The algorithm is presented below. Note: It is a dual of the algorithm for computing one “3-stable” triangle  $\triangle v_i v_j v_k$  in [7], where “3-stable” is a similar notion defined in that paper.

**Step 1.** Choose  $a$  to be an arbitrary edge of  $P$ ; say  $a = e_1$ . Find  $b, c$  so that  $\triangle abc$  is the smallest all-flush triangle rooted at  $a$ . Specifically, enumerate an edge  $b$  in clockwise and compute  $c_b = \text{OPT}_{a,b}$  and then select  $b$  so that  $\triangle abc_b$  is minimum. Using the bi-monotonicity of  $\{\text{OPT}_{a,b}\}$  (Lemma 5) with the unimodality of  $\text{Area}(\triangle abc)$  for fixed  $a, b$  (Lemma 4), the computation of  $c_b$  costs amortized  $O(1)$  time, hence the entire running time is  $O(n)$ .

In triangle  $\triangle abc$ , the edges  $b, c$  must be stable. (Otherwise  $\triangle abc$  is not the smallest all-flush triangle rooted at  $a$ .) If  $a$  is also stable (which can be determined in  $O(1)$  time using Lemma 4), we have already found a 3-stable triangle and we proceed to the next section.

Here, we consider the other case where  $a$  is not stable. Assume that  $\text{Area}(\triangle(a+1)bc) < \text{Area}(\triangle abc)$ . Otherwise,  $\text{Area}(\triangle(a-1)bc) < \text{Area}(\triangle abc)$  and is symmetric.

**Step 2.** This step is presented in Algorithm 1.

To distinguish, we denote the value of the three pointers  $(a, b, c)$  at the end phase of this algorithm by  $(a_1, b_1, c_1)$ ; and the value at the beginning phase by  $(a_0, b_0, c_0)$ .

► **Observation 6.** Edges  $b_1, c_1$  are stable in  $\triangle a_1 b_1 c_1$ .

► **Observation 7.**  $\text{Area}(\triangle a_1 b_1 c_1) < \text{Area}(\triangle(a_1 - 1) b_1 c_1)$ . (Note that  $a_1 - 1 = a_0$ .)

The trivial proofs of the above observations are deferred to Appendix A.

**Step 3.** So far, we obtain  $\triangle a_1 b_1 c_1$  where  $b_1, c_1$  are stable. If  $a_1$  is also stable,  $\triangle a_1 b_1 c_1$  is 3-stable and we proceed to next section. Now, consider the case where  $a_1$  is not stable. Because  $a_1$  is not stable,  $\text{Area}(\triangle a_1 b_1 c_1) > \text{Area}(\triangle(a_1 + 1) b_1 c_1)$  or  $\text{Area}(\triangle a_1 b_1 c_1) > \text{Area}(\triangle(a_1 -$

```

1  $a \leftarrow a + 1$ ;
2 repeat
3   while  $\text{Area}(\triangle a(b+1)c) < \text{Area}(\triangle abc)$  do
4      $b \leftarrow b + 1$ ;
5   end
6   while  $\text{Area}(\triangle ab(c+1)) < \text{Area}(\triangle abc)$  do
7      $c \leftarrow c + 1$ ;
8   end
9 until  $\text{Area}(\triangle a(b+1)c) \geq \text{Area}(\triangle abc)$  and  $\text{Area}(\triangle ab(c+1)) \geq \text{Area}(\triangle abc)$ ;

```

**Algorithm 1:** Algorithm for Step 2

$1)b_1c_1$ ) due to Lemma 4. Further applying Observation 7, we get  $\text{Area}(\triangle a_1b_1c_1) > \text{Area}(\triangle (a_1+1)b_1c_1)$ . We call Algorithm 1 once again with initial value  $(a_1, b_1, c_1)$  and terminal value  $(a_2, b_2, c_2)$ , and repeat such a process until  $\triangle a_i b_i c_i$  is 3-stable for some integer  $i$ .

**Analysis of correctness and running time.** At every change of  $a, b, c$  in Algorithm 1,  $\text{Area}(\triangle abc)$  strictly decreases. Therefore, the above process terminates eventually. Moreover, it runs in  $O(n)$  time because pointers  $a, b, c$  can only move in the clockwise direction and  $a$  cannot return to  $a_0$  - because  $\triangle a_0 b_0 c_0$  is the smallest all-flush triangle rooted at  $a_0$ .

### 3 Compute all the 3-stable triangles in $O(n \log n)$ time

In this section, we present our first algorithm for computing all 3-stable triangles based on the Rotate-and-Kill framework. It runs in  $O(n \log n)$  time, which is as efficient as any previous algorithms. However, it seems unable to be improved to linear time. Our linear time algorithm given in the next section applies the same framework together with several more tricks, which does not depend on any observations or results in this section.

In the following, for edge pair  $(e_j, e_k)$  such that  $e_j \prec e_k$ , we define a set  $Q_{j,k}$  which contains all the edges  $e_i$  for which  $e_j$  and  $e_k$  are stable in  $\triangle e_i e_j e_k$ . For convenience, we use  $<$  and  $\leq$  to indicate the clockwise order among the edges in  $\{e_k, e_{k+1}, \dots, e_j\}$ .

► **Definition 8.** Assume  $e_j \prec e_k$ , define

- $sX_{j,k}$  to be the clockwise first edge  $e_i$ , such that  $\text{Area}(\triangle e_i e_j e_k) \leq \text{Area}(\triangle e_i e_{j-1} e_k)$ ;
- $tX_{j,k}$  to be the clockwise last edge  $e_i$ , such that  $\text{Area}(\triangle e_i e_j e_k) \leq \text{Area}(\triangle e_i e_{j+1} e_k)$ ;
- $sY_{j,k}$  to be the clockwise first edge  $e_i$ , such that  $\text{Area}(\triangle e_i e_j e_k) \leq \text{Area}(\triangle e_i e_j e_{k-1})$ ;
- $tY_{j,k}$  to be the clockwise last edge  $e_i$ , such that  $\text{Area}(\triangle e_i e_j e_k) \leq \text{Area}(\triangle e_i e_j e_{k+1})$ .

► **Observation 9.**

1.  $sX_{j,k} \leq tX_{j,k} + 1$  and it is possible that the equality holds.
2.  $sY_{j,k} \leq tY_{j,k} + 1$  and it is possible that the equality holds.

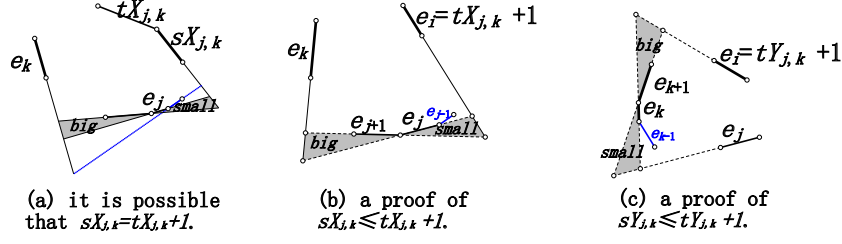
The trivial proof of Observation 9 is omitted; see Figure 5 for an illustration.

► **Definition 10.** Assume  $e_j \prec e_k$ , define

$$X_{j,k} = \begin{cases} \{sX_{j,k}, \dots, tX_{j,k}\}, & sX_{j,k} \leq tX_{j,k}; \\ \emptyset, & sX_{j,k} = tX_{j,k} + 1. \end{cases} \quad (1)$$

$$Y_{j,k} = \begin{cases} \{sY_{j,k}, \dots, tY_{j,k}\}, & sY_{j,k} \leq tY_{j,k}; \\ \emptyset, & sY_{j,k} = tY_{j,k} + 1. \end{cases} \quad (2)$$

$$Q_{j,k} = X_{j,k} \cap Y_{j,k} \quad (3)$$

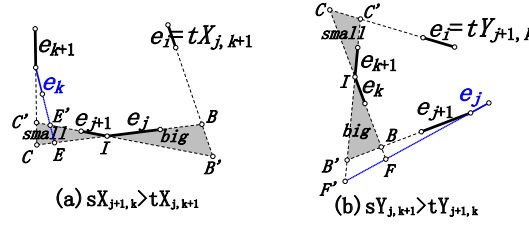


■ **Figure 5** Illustration of Observation 9.

Note:  $X_{j,k}$  indicates the set of  $e_i$  for which  $e_j$  is stable in  $\triangle e_i e_j e_k$ ;  $Y_{j,k}$  indicates the set of  $e_i$  for which  $e_k$  is stable in  $\triangle e_i e_j e_k$ ; and so  $Q_{j,k}$  is the set of  $e_i$  for which both  $e_j, e_k$  are stable.

► **Observation 11.**

1. The interval  $X_{j+1,k}$  is strictly after  $X_{j,k+1}$  in clockwise. Formally,  $sX_{j+1,k} > tX_{j,k+1}$ .
2. The interval  $Y_{j,k+1}$  is strictly after  $Y_{j+1,k}$  in clockwise. Formally,  $sY_{j,k+1} > tY_{j+1,k}$ .



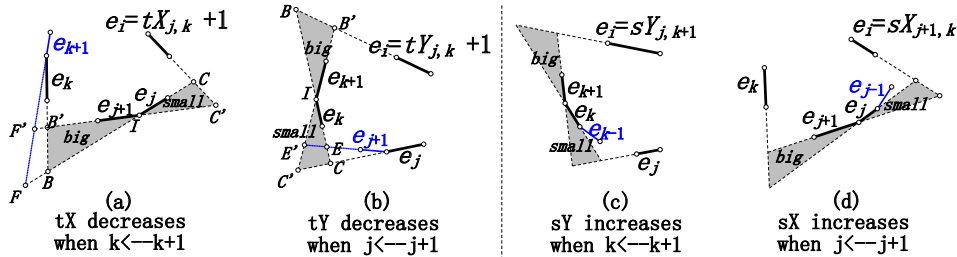
■ **Figure 6** Illustration of the proof of Observation 11.

**Proof.** 1. See Figure 6 (a). Denote  $e_i = tX_{j,k+1}$ . Let  $I, B, B', C, C', E, E'$  be the intersections as illustrated in the figure. By definition of  $tX_{j,k+1}$ , we have  $\text{Area}(\triangle e_i e_j e_{k+1}) \leq \text{Area}(\triangle e_i e_{j+1} e_{k+1})$ . Equivalently,  $\text{Area}(\triangle ICC') \leq \text{Area}(\triangle IBB')$ . Therefore,  $\text{Area}(\triangle IEE') < \text{Area}(\triangle IBB')$ . Equivalently,  $\text{Area}(\triangle e_i e_j e_k) < \text{Area}(\triangle e_i e_{j+1} e_k)$ , which implies  $sX_{j+1,k} > e_i$ .

2. The proof of Claim 2 is symmetric and omitted; see Figure 6 (b). ◀

► **Observation 12** (Monotonicties of  $\{X_{j,k}\}$  and  $\{Y_{j,k}\}$ ).

1.  $tX_{j,k+1} \leq tX_{j,k}$ ; 2.  $tY_{j+1,k} \leq tY_{j,k}$ ; 3.  $sY_{j,k+1} \geq sY_{j,k}$  4.  $sX_{j+1,k} \geq sX_{j,k}$ .



■ **Figure 7** Illustration of the proof of Observation 12.

**Proof.** 1. See Figure 7 (a). Let  $e_i = tX_{j,k} + 1$ . By definition of  $tX_{j,k}$ , we have  $\text{Area}(\triangle e_i e_{j+1} e_k) < \text{Area}(\triangle e_i e_j e_k)$ . Equivalently,  $\text{Area}(\triangle ICC') < \text{Area}(\triangle IBB')$ . Therefore,  $\text{Area}(\triangle ICC') < \text{Area}(\triangle IFF')$ . Equivalently,  $\text{Area}(\triangle e_i e_{j+1} e_{k+1}) < \text{Area}(\triangle e_i e_j e_{k+1})$ . So  $tX_{j,k+1} < e_i$ .



Claim 2 is symmetric to 1. Claim 4 is symmetric to 3. We omit their proofs.

3. See Figure 7 (c). Let  $e_i = sY_{j,k+1}$ . By definition of  $sY_{j,k+1}$ , we have  $\text{Area}(\triangle e_i e_j e_{k+1}) \leq \text{Area}(\triangle e_i e_j e_k)$ . Applying the unimodality stated in Lemma 4, we have  $\text{Area}(\triangle e_i e_j e_k) < \text{Area}(\triangle e_i e_j e_{k-1})$ . This further implies  $sY_{j,k} \leq e_i$  according to the definition of  $sY_{j,k}$ .  $\blacktriangleleft$

- **Lemma 13. 1.** *At least one is true: (a)  $sY_{j,k+1} > tX_{j,k+1}$ ; or (b)  $sX_{j+1,k} > tY_{j+1,k}$ .*  
 2. *If (a) happens, we claim that  $Q_{j,k+1}, Q_{j,k+2}, \dots, Q_{j,k+\Delta}$  are all empty.*  
 3. *If (b) happens, we claim that  $Q_{j+1,k}, Q_{j+2,k}, \dots, Q_{j+\Delta,k}$  are all empty.*

**Proof.** 1. Consider the four intervals  $X = X_{j,k+1}, Y = Y_{j,k+1}, X' = X_{j+1,k}, Y' = Y_{j+1,k}$ . Due to Observation 11,  $X'$  is strictly after  $X$ , and  $Y$  is strictly after  $Y'$ . Therefore, at least one is true:  $Y$  is strictly after  $X$ ; namely, (a); or  $X'$  is strictly after  $Y'$ ; namely, (b).

2. Assume  $sY_{j,k+1} > tX_{j,k+1}$ . Applying Observation 12 (in particular, Inequality 1 and 3), we know  $sY_{j,k+2} > tX_{j,k+2}, \dots, sY_{j,k+\Delta} > tX_{j,k+\Delta}$ . So,  $\{Q_{j,k+\delta} \mid \delta \geq 1\}$  are all empty.

3. Assume  $sX_{j+1,k} > tY_{j+1,k}$ . Applying Observation 12 (in particular, Inequality 2 and 4), we know  $sX_{j+2,k} > tY_{j+2,k}, \dots, sX_{j+\Delta,k} > tY_{j+\Delta,k}$ . So,  $\{Q_{j+\delta,k} \mid \delta \geq 1\}$  are all empty.  $\blacktriangleleft$

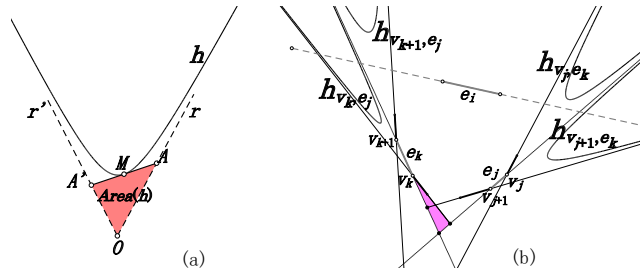
We can use (a) (or (b)) to be the decision-condition of the Rotate-and-Kill process. Recall this process in Subsection 1.2 and assume that  $(b, c) = (e_j, e_k)$  now. If (a) happens, we obtain that  $(e_j, e_{k+1}), (e_j, e_{k+2}), \dots, (e_j, e_{k+\Delta})$  are dead by Lemma 13.2, thus we can safely kill  $j$ . Otherwise (b) must hold according to Lemma 13.1, and we obtain that  $(e_{j+1}, e_k), (e_{j+2}, e_k), \dots, (e_{j+\Delta}, e_k)$  are dead by Lemma 13.3, thus we can safely kill  $k$ . The algorithm runs in  $O(n \log n)$  time because (a) (or (b)) can easily be determined in  $O(\log n)$  time -  $sX_{j,k}, tX_{j,k}, sY_{j,k}, tY_{j,k}$  can be computed by binary searches using Definition 8.

#### 4 Compute all the 3-stable triangles in $O(n)$ time

To design a linear time algorithm, we need a decision-condition which can guide us to kill  $j$  or kill  $k$  and which can be computed in  $O(1)$  time. We find such a condition right below.

► **Observation 14.** *Assume  $r, r'$  are rays at  $O$  and are asymptotes of a fixed hyperbola branch  $h$ . See Figure 8 (a). Let  $A, A'$  be points on  $r, r'$  so that  $AA'$  is tangent to  $h$ . Then, the area of  $\triangle OAA'$  is a constant. This area is defined as the triangle-area of  $h$ , denoted by  $\text{Area}(h)$ . Moreover, the triangle-area of a hyperbola is the triangle-area of either of its branch.*

Consider any edge  $e_j$  and vertex  $v_k$  so that  $e_j \notin \{e_{k-1}, e_k\}$ . See Figure 8 (b). Let  $T$  denote the triangle bounded by  $\ell_j, \ell_{k-1}, \ell_k$ . There is a unique hyperbola which admit  $\ell_{k-1}, \ell_k$  as asymptotes and has triangle-area as much as  $\text{Area}(T)$ . One branch of this hyperbola is tangent to  $T$ , whereas the other branch is denoted by  $h_{v_k, e_j}$ .



■ **Figure 8** Illustration of Observation 14 and Observation 15



► **Observation 15.** If  $e_j, e_k$  are stable in an all-flush triangle  $\triangle e_i e_j e_k$ , then

1.  $\ell_i$  must intersect  $h_{v_k, e_j}$ , and it must avoid  $h_{v_{k+1}, e_j}$ .
2.  $\ell_i$  must intersect  $h_{v_{j+1}, e_k}$ , and it must avoid  $h_{v_j, e_k}$ .

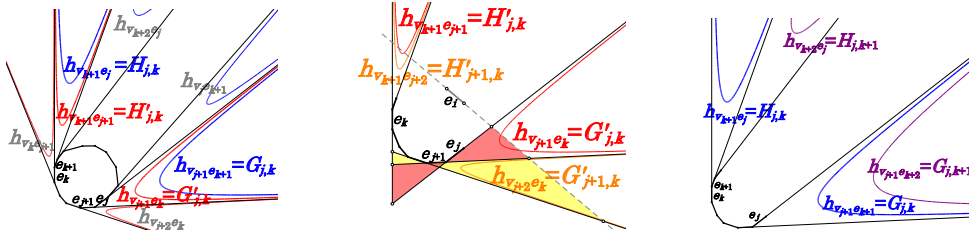
Note: “avoid” means “be disjoint with or tangent to”.

Consider any edge pair  $(e_j, e_k)$  such that  $e_j \prec e_k$ , as shown in Figure 9. Let  $G_{j,k}, H_{j,k}$  denote  $h_{v_{j+1}, e_{k+1}}, h_{v_{k+1}, e_j}$  for short. Let  $G'_{j,k}, H'_{j,k}$  denote  $h_{v_{j+1}, e_k}, h_{v_{k+1}, e_{j+1}}$  for short.

► **Observation 16.** Assume  $e_j \prec e_k$  and  $e_i$  is any edge in  $\{e_{k+1}, \dots, e_{j-1}\}$ .

1. If  $\ell_i$  avoids  $H'_{j+1,k}$ , it will also avoid  $H'_{j,k}$ .
2. If  $\ell_i$  avoids  $G'_{j+1,k}$ , it will also avoid  $G'_{j,k}$ .
3. If  $\ell_i$  intersects  $H_{j,k+1}$ , it will also intersects  $H_{j,k}$ .
4. If  $\ell_i$  intersects  $G_{j,k+1}$ , it will also intersects  $G_{j,k}$ .

**Proof.** See the middle picture of Figure 9. 1. This is because  $H'_{j,k}$  lies in the area bounded by  $H'_{j+1,k}$ . 2. Suppose to the opposite that  $\ell_i$  does not avoid  $G'_{j,k}$ . Then,  $\ell_i$  intersects and is not tangent to  $G'_{j,k}$ . Then  $\text{Area}(\triangle e_i e_{j+1} e_k) > \text{Area}(\triangle e_i e_j e_k)$ . Applying the unimodality in Lemma 4, we have  $\text{Area}(\triangle e_i e_{j+2} e_k) > \text{Area}(\triangle e_i e_{j+1} e_k)$ . This implies that  $\ell_i$  intersects and is not tangent to  $G'_{j+1,k}$ , namely,  $\ell_i$  does not avoid  $G'_{j+1,k}$ . Contradiction. The last two claims are symmetric to the first two; proof omitted; see the last picture of Figure 9. ◀



■ **Figure 9** Illustration of Observation 16 and Lemma 17

► **Lemma 17.** Assume  $e_j \prec e_k$ .

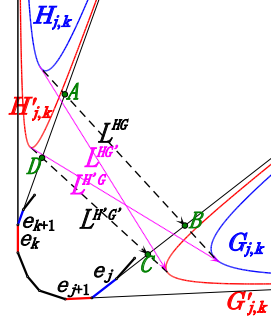
1.  $(e_j, e_{k+1}), (e_j, e_{k+2}), \dots, (e_j, e_{k+\Delta})$  are all dead when the following condition holds:  
(I) There is no edge  $e_i \in \{e_{k+1}, \dots, e_j\}$  such that  $\ell_i$  intersects  $H_{j,k}, G_{j,k}$  simultaneously.
2.  $(e_{j+1}, e_k), (e_{j+2}, e_k), \dots, (e_{j+\Delta}, e_k)$  are all dead when the following condition holds:  
(II) There is no edge  $e_i \in \{e_{k+1}, \dots, e_j\}$  such that  $\ell_i$  avoids  $H'_{j,k}, G'_{j,k}$  simultaneously.

**Proof.** 1. Suppose to the opposite that  $(e_j, e_{k+\delta})$  is not dead. This means there is  $e_i \in \{e_{k+1}, \dots, e_j\}$  such that  $\triangle e_i e_j e_{k+\delta}$  is 3-stable. Applying Observation 15,  $\ell_i$  intersects  $H_{j,k+\delta-1}$  and  $G_{j,k+\delta-1}$ . Further applying Observation 16,  $\ell_i$  intersects  $H_{j,k}$  and  $G_{j,k}$ .

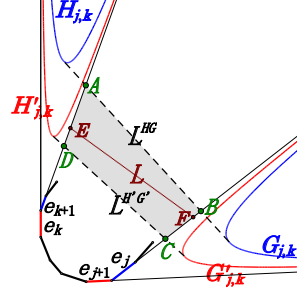
2. Suppose to the opposite that  $(e_{j+\delta}, e_k)$  is not dead. This means there is  $e_i \in \{e_{k+1}, \dots, e_j\}$  such that  $\triangle e_i e_{j+\delta} e_k$  is 3-stable. Applying Observation 15,  $\ell_i$  avoids  $H'_{j+\delta-1,k}$  and  $G'_{j+\delta-1,k}$ . Further applying Observation 16,  $\ell_i$  avoids  $H'_{j,k}$  and  $G'_{j,k}$ . ◀

Lemma 17 provides a condition (I) to kill  $j$  and a condition (II) to kill  $k$ . Unfortunately, these conditions cannot be applied directly because they are expensive to compute. The next lemma provides simple conditions under which the above conditions hold.

Denote by  $L_{j,k}^{HG}$  the common tangent of  $H_{j,k}$  and  $G_{j,k}$ , and denote the other three common tangents by  $L_{j,k}^{HG'}, L_{j,k}^{H'G}$  and  $L_{j,k}^{H'G'}$ , as shown in Figure 10. Omit  $j, k$  when they are clear.



■ **Figure 10** Four common-tangents.



■ **Figure 11** Kill by comparing  $P$  with  $L$ .

► **Lemma 18.** Let  $A, B, C, D$  respectively denote the intersections  $L^{HG} \cap \ell_{k+1}$ ,  $L^{HG} \cap \ell_j$ ,  $L^{H'G'} \cap \ell_j$  and  $L^{H'G'} \cap \ell_{k+1}$ . Assume points  $E, F$  lies in the open segments  $\overline{AD}, \overline{BC}$  and  $L$  is the directed line connecting  $E$  and  $F$ , which is directed from  $E$  to  $F$ . See Figure 11. We claim that (I) holds when  $P$  lies on the right of  $L$ , and (II) holds otherwise.

**Proof.** The former part is obvious from the figure. When  $P$  lies on the right of  $L$ , no edge of  $P$  can have its extended line intersect  $H_{j,k}, G'_{j,k}$ . We prove the otherwise part by indirect method. Suppose (II) is false. There must be an edge  $e_i$  such that  $\ell_i$  avoid  $H'_{j,k}$  and  $G'_{j,k}$ . This means  $P$  lies on the right of  $\overrightarrow{DC}$ , which simply implies that  $P$  lies on the right of  $L$ . ◀

For convenience, we assume that the four common tangents introduced above are **directed** lines. The direction of  $L^{HG}$  is from  $A$  to  $B$ ; the direction of  $L^{H'G'}$  is from  $D$  to  $C$ ; the direction of  $L^{HG'}$  is from its tangent point with  $H_{j,k}$  to its tangent point with  $G'_{j,k}$ ; and the direction of  $L^{H'G}$  is from its tangent point with  $H'_{j,k}$  to its tangent point with  $G_{j,k}$ .

For any directed line  $L$ , let  $d(L)$  denote its direction, which is an angle in  $[0, 2\pi)$ . We define the direction so that  $d(\overrightarrow{OA})$  increases when  $A$  rotate in clockwise around  $O$ .

We can describe our final algorithm now. Recall its framework in Subsection 1.2.

In each iteration, we are given a pair of edge  $(b, c) = (e_j, e_k)$ .

First, we select a direction  $d \in [d(L_{j,k}^{H'G}), d(L_{j,k}^{HG'})]$ . (See Figure 10 for  $L_{j,k}^{H'G}$  and  $L_{j,k}^{HG'}$ .)

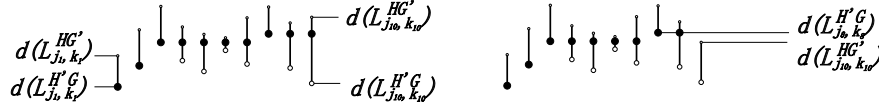
Then, we find any line  $L$  with direction  $d$  so that the intersection  $E, F$  lies in  $\overline{AB}$  and  $\overline{CD}$  where  $E = L \cap \ell_{k+1}$  and  $F = L \cap \ell_j$  as in Lemma 18. We also compute the unique supporting line  $L'$  of  $P$  with direction  $d$  so that  $P$  touches  $L'$  and lies on the right of  $L'$ .

Compare  $L'$  with  $L$ . If  $L'$  lies on the right of  $L$ , we know  $P$  lies on the right of  $L$ , hence (I) holds by Lemma 18, and we kill  $j$  according to Lemma 17.1. Otherwise,  $P$  does not lie on the right of  $L$ , hence (II) holds by Lemma 18, and we kill  $k$  according to Lemma 17.2.

The computation of  $L$  only takes  $O(1)$  time. The computation of  $L'$  takes amortized  $O(1)$  time if we can guarantee that *the variable  $d$  keeps increasing during the entire algorithm*. (More precisely, we mean that  $d$  will be increased by at most  $2\pi$  during the algorithm.) Fortunately, this monotonicity can be guaranteed as long as we use the following rule to

choose  $d$ :  $d_{\text{this-iteration}} = \begin{cases} d_{\text{previous-iteration}}, & d_{\text{previous-iteration}} \in [d(L_{j,k}^{H'G}), d(L_{j,k}^{HG'})]; \\ d(L_{j,k}^{H'G}), & \text{otherwise.} \end{cases}$

Since  $j$  and  $k$  keeps (non-strictly) increasing during our algorithm, the monotonicity of  $d$  follows from the following lemma - see illustration in Figure 12.



■ **Figure 12** The left picture shows how  $d$  is increased in each iteration according to the above rule. The right picture shows that we cannot get the monotonicity of  $d$  if Lemma 19 was not true.

► **Lemma 19.** Assume  $j' \geq j$  and  $k' \geq k$ . Then  $d(L_{j',k'}^{HG'}) \geq d(L_{j,k}^{H'G})$ .<sup>1</sup>

**Proof.** Throughout this proof, assume that  $A = \ell_{j+1} \cap \ell_{k+1}$ ,  $B = \ell_{j'} \cap \ell_{k'}$ , and

$$M_1 = \begin{cases} \text{undefined,} & j' = j; \\ v_{j'+1}, & j' = j+1; \\ \ell_{j+1} \cap \ell_{j'}, & j' \geq j+2 \end{cases} \text{ and } M_2 = \begin{cases} \text{undefined,} & k' = k; \\ v_{k'+1}, & k' = k+1; \\ \ell_{k+1} \cap \ell_{k'}, & k' \geq k+2 \end{cases}.$$

First, consider the easiest case where  $j' > j$  and  $k' > k$ . See Figure 13.

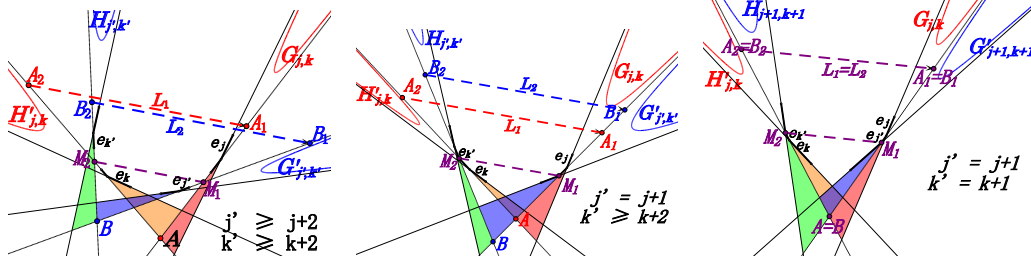
Denote the reflections of  $A$  around  $M_1, M_2$  by  $A_1, A_2$  respectively. Denote the reflections of  $B$  around  $M_1, M_2$  by  $B_1, B_2$  respectively. Let  $L_1 = A_2A_1$  and  $L_2 = B_2B_1$ .

We state the following equalities or inequalities which together implies our result.

(i)  $d(L_1) > d(L_{j,k}^{H'G})$ . (ii)  $d(L_{j',k'}^{HG'}) > d(L_2)$ . (iii)  $d(L_1) = d(M_2M_1) = d(L_2)$ .

(iii) is trivial. (ii) is symmetric to (i). We prove (i) in the following.

Since  $|AM_2| = |A_2M_2|$ , we know  $|Av_{k+1}| < |A_2v_{k+1}|$ . This means the triangle bounded by  $\ell_k, \ell_{k+1}, \ell_{j+1}$  is smaller than the triangle bounded by  $\ell_k, \ell_{k+1}, L_1$ . This means  $L_1$  intersects  $H'_{j,k}$ . Similarly, we can prove that  $L_1$  avoid  $G_{j,k}$ . Together, we get  $d(L_1) > d(L_{j,k}^{H'G})$ .

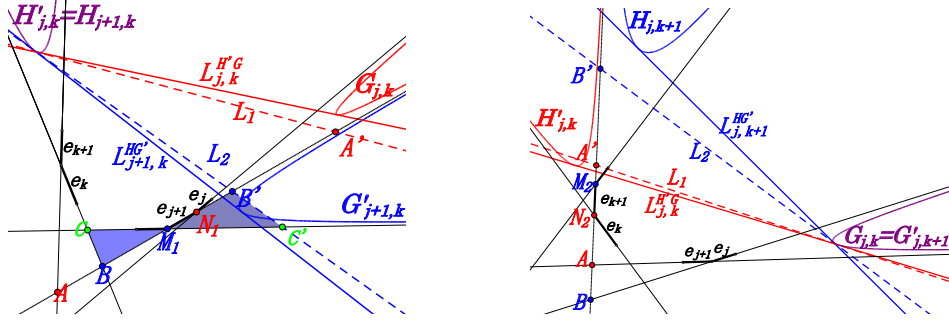


■ **Figure 13** Proof of Lemma 19 - part I.

Next, we consider four cases. (We remark that the last two cases are nontrivial.)

- Case 1  $j' = j+1, k' = k$ . See the left picture of Figure 14. Note that  $H'_{j,k} = H_{j+1,k}$ . Denote  $N_1 = v_{j+1}$ . Let  $A'$  be the reflection of  $A$  around  $N_1$  and  $B'$  the reflection of  $B$  around  $M_1$ . Let  $L_1$  be the tangent line of  $H'_{j,k}$  that passes through  $A'$ , and  $L_2$  the tangent line of  $H_{j+1,k}$  that passes through  $B'$ . Applying some analysis similar to that used in the previous case, we obtain the inequalities (i) and (ii). Moreover, since  $B', A'$  lie in order on  $\overrightarrow{M_2M_1}$ , we obtain  $d(L_2) > d(L_1)$ . Altogether, we get  $d(L_{j',k'}^{HG'}) \geq d(L_{j,k}^{H'G})$ .
- Case 2  $j' = j, k' = k+1$ . Symmetric to Case 1 (see the right picture of Figure 14).
- Case 3  $j' \geq j+2, k' = k$ . See Figure 15 (a). (Hint: This case is more difficult because  $H_{j',k'}$  is now “below”  $H'_{j,k}$  as shown in the figure; this proof contains several more tricks.)
- Let  $A', B'$  be the reflection of  $A, B$  around  $M_1$  respectively. Let  $L_1$  be the tangent line of  $H'_{j,k}$  that passes through  $A'$ , and  $L_2$  the tangent line of  $H_{j',k'}$  that passes through  $B'$ . As the previous cases, it reduces to show that  $d(L_2) > d(L_1)$ .

<sup>1</sup> For conciseness and ease of presentation, we do not state this lemma rigorously.

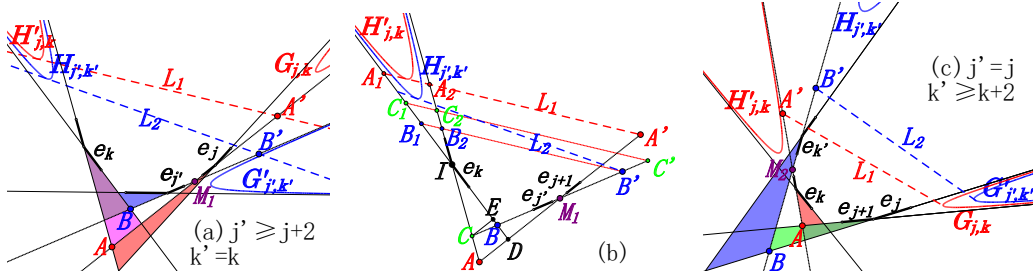


■ **Figure 14** Proof of Lemma 19 - part II.

See Figure 15 (b). Denote  $I = v_{k+1}$ . Make a parallel line of  $L_1$  at point  $B'$ , and assume it intersects  $\ell_k, \ell_{k+1}$  at  $B_1, B_2$  respectively. It reduces to show that  $\text{Area}(\triangle IB_1B_2) < \text{Area}(H'_{j',k'})$ . (Here, recall the triangle-area of hyperbola defined in Observation 14.) In other words, it reduces to prove  $\text{Area}(\triangle IB_1B_2) < \text{Area}(\triangle IBC)$ , where  $C = \ell_{k+1} \cap \ell_{j'}$ .

Denote by  $C'$  the reflection of  $C$  around  $M_1$ . Make a parallel line of  $L_1$  at  $C'$  and assume it intersects  $\ell_k, \ell_{k+1}$  at  $C_1, C_2$  respectively. Denote  $D = \ell_{j+1} \cap \ell_k$ . Assume  $E$  is the point on  $\ell_k$  so that  $\overline{CE}$  is parallel to  $\overline{AD}$ . Apparently,  $\text{Area}(\triangle IB_1B_2) < \text{Area}(\triangle IC_1C_2)$  and  $\text{Area}(\triangle IEC) < \text{Area}(\triangle IBC)$ . Therefore, it further reduces to prove that  $\text{Area}(\triangle IC_1C_2) < \text{Area}(\triangle IEC)$ .

Assume that  $L_1$  intersects  $\ell_k, \ell_{k+1}$  at  $A_1, A_2$ . Since  $L_1$  is tangent to  $H'_{j,k}$ , we have (I):  $\text{Area}(\triangle IA_1A_2) = \text{Area}(\triangle IDA)$ . This further implies (II):  $|A_2| < |IA|$ . Moreover, notice that segment  $A'C'$  is a translate of segment  $CA$ , we have: (III)  $|AC| = |A_2C_2|$ . Combining facts (I), (II) and (III), it simply follows that  $\text{Area}(\triangle IC_1C_2) < \text{Area}(\triangle IEC)$ .



■ **Figure 15** Proof of Lemma 19 - part III.

Case 4  $j' = j, k' \geq k + 2$ . Totally symmetric to Case 3 (see Figure 15 (c)).

► **Remark.** The reader may wonder whether  $d(L_{j,k}^{HG})$  (or,  $d(L_{j,k}^{H'G'})$ ) is monotone with respect to  $j$  and  $k$ . If so, we can simply choose  $d = d(L_{j,k}^{HG})$  (or,  $d = d(L_{j,k}^{H'G'})$ ) at each iteration and thus simplify the algorithm. We disprove it by counterexamples in Appendix C.

### Acknowledgement

The authors appreciate the developers of Geometer's Sketchpad®.

---

**References**


---

- 1 A. Aggarwal, J.S. Chang, and C.K. Yap. Minimum area circumscribing polygons. *The Visual Computer*, 1(2):112–117, Aug 1985. doi:10.1007/BF01898354.
- 2 A. Aggarwal, B. Schieber, and T. Tokuyama. Finding a minimum-weight k-link path in graphs with the concave monge property and applications. *Discrete & Computational Geometry*, 12(1):263–280, 1994.
- 3 J. E. Boyce, D. P. Dobkin, R. L. (Scot) Drysdale, III, and L. J. Guibas. Finding extremal polygons. In *14th Symposium on Theory of Computing*, pages 282–289, 1982.
- 4 S. Chandran and D. M. Mount. A paraellel algorithm for enclosed and enclosing triangles. *International Journal of Computational Geometry & Applications*, 02(02):191–214, 1992. doi:10.1142/S0218195992000123.
- 5 D. P. Dobkin and L. Snyder. On a general method for maximizing and minimizing among certain geometric problems. In *20th Annual Symposium on Foundations of Computer Science*, pages 9–17, Oct 1979. doi:10.1109/SFCS.1979.28.
- 6 K. Jin. Maximal parallelograms in convex polygons - a novel geometric structure. *CoRR*, abs/1512.03897, 2015. URL: <http://arxiv.org/abs/1512.03897>.
- 7 K. Jin. Maximal area triangles in a convex polygon. *CoRR*, abs/1707.04071, 2017. URL: <http://arxiv.org/abs/1707.04071>.
- 8 V. Keikha, M. Löffler, J. Urhausen, and I. v. d. Hoog. Maximum-area triangle in a convex polygon, revisited. *CoRR*, abs/1705.11035, 2017.
- 9 V. Klee and M. C. Laskowski. Finding the smallest triangles containing a given convex polygon. *Journal of Algorithms*, 6(3):359 – 375, 1985. doi:[https://doi.org/10.1016/0196-6774\(85\)90005-7](https://doi.org/10.1016/0196-6774(85)90005-7).
- 10 J. S.B. Mitchell and V. Polishchuk. Minimum-perimeter enclosures. *Information Processing Letters*, 107(3):120 – 124, 2008. doi:<https://doi.org/10.1016/j.ipl.2008.02.007>.
- 11 J. O’Rourke, A. Aggarwal, S. Maddila, and M. Baldwin. An optimal algorithm for finding minimal enclosing triangles. *Journal of Algorithms*, 7(2):258 – 269, 1986. doi:[http://dx.doi.org/10.1016/0196-6774\(86\)90007-6](http://dx.doi.org/10.1016/0196-6774(86)90007-6).
- 12 B. Schieber. Computing a minimum-weight k-link path in graphs with the concave monge property. In *Proceedings of the Sixth Annual ACM-SIAM Symposium on Discrete Algorithms*, SODA ’95, pages 405–411. Society for Industrial and Applied Mathematics, 1995.

## A

**Proofs omitted in Section 2**

**Proof of Observation 6.** We shall prove that  $b_1, c_1$  are stable in  $\triangle a_1 b_1 c_1$ .

It reduces to prove the following inequalities.

- (1)  $\text{Area}(\triangle a_1(b_1 - 1)c_1) \geq \text{Area}(\triangle a_1 b_1 c_1)$ .
- (2)  $\text{Area}(\triangle a_1(b_1 + 1)c_1) \geq \text{Area}(\triangle a_1 b_1 c_1)$ .
- (3)  $\text{Area}(\triangle a_1 b_1(c_1 - 1)) \geq \text{Area}(\triangle a_1 b_1 c_1)$ .
- (4)  $\text{Area}(\triangle a_1 b_1(c_1 + 1)) \geq \text{Area}(\triangle a_1 b_1 c_1)$ .

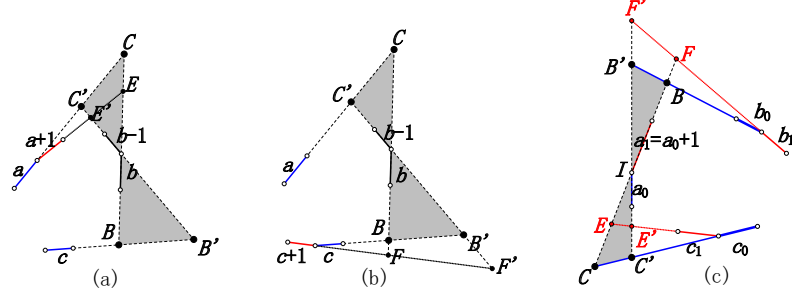
Due to the termination condition of Algorithm 1, (2) and (4) hold. In the following we point out two facts that hold throughout Algorithm 1, which respectively imply (1) and (3).

- (i)  $\text{Area}(\triangle(a(b - 1)c)) \geq \text{Area}(\triangle abc)$ .
- (ii)  $\text{Area}(\triangle(ab(c - 1))) \geq \text{Area}(\triangle abc)$ .

(i) follows from the following four arguments. The proof of (ii) is symmetric and omitted.

- i.0 (i) holds at the beginning, because  $b_0$  is stable in  $\triangle a_0 b_0 c_0$ .
- i.1 When  $b$  is to be increased by 1 at Line 4 of Algorithm 1, (i) will hold after this increasing sentence according to the condition at Line 3 of Algorithm 1.

- i.2 When  $a$  is to be increased by 1 at Line 1 of Algorithm 1, (i) will still hold. This is simply illustrated in Figure 16 (a).
- i.3 When  $c$  is to be increased by 1 at Line 7 of Algorithm 1, (i) will still hold. This is simply illustrated in Figure 16 (b).
- The proofs of i.2 and i.3 are similar to the proof of Lemma 5 and are omitted. ◀



■ **Figure 16** Illustration of the proof of Observation 6 and Observation 7.

**Proof of Observation 7.** We shall prove that  $\text{Area}(\triangle a_1 b_1 c_1) < \text{Area}(\triangle (a_1 - 1) b_1 c_1)$ . See figure 16 (c). Let  $I, B, B', C, C', E, E', F, F'$  denote the intersections as shown in figure.

According to the assumption entering Step 2, we have  $\text{Area}(\triangle a_1 b_0 c_0) < \text{Area}(\triangle (a_1 - 1) b_0 c_0)$ . This means (1)  $\text{Area}(\triangle ICC') < \text{Area}(\triangle IBB')$ .

Moreover, since pointers  $b, c$  only increase during Algorithm 1, we get the following monotonicities:  $b_1 \geq b_0$  in clockwise in list  $a_1, \dots, a_0$  and  $c_1 \geq c_0$  in clockwise in list  $a_1, \dots, a_0$ . This means (2)  $\text{Area}(\triangle IEE') < \text{Area}(\triangle ICC')$  and (3)  $\text{Area}(\triangle IBB') < \text{Area}(\triangle IFF')$ .

Combine (1), (2), and (3). We get  $\text{Area}(\triangle IEE') < \text{Area}(\triangle IFF')$ .

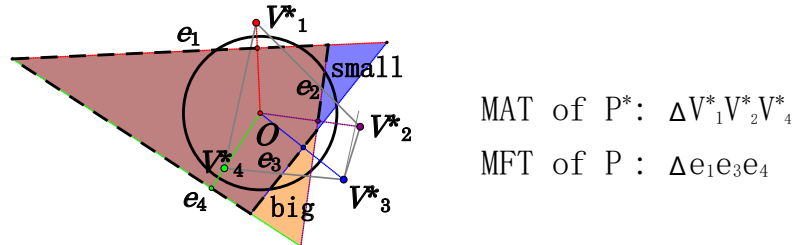
Equivalently,  $\text{Area}(\triangle a_1 b_1 c_1) < \text{Area}(\triangle (a_1 - 1) b_1 c_1)$ . ◀

## B A wrong reduction from MFT to MAT

It is claimed in [2, 12] that computing the MFT is the dual problem of computing the MAT. We believe that this is only from the combinatorial perspective. In this appendix we consider an intuitive but wrong reduction from MFT to MAT. The reduction is as follows.

Assume the  $n$  edges of  $P$  are  $e_1, \dots, e_n$ . Let  $P^*$  denote the dual polygon of  $P$  at some point  $O$ , whose vertices are  $V_1^*, \dots, V_n^*$ . To compute the MFT circumscribing  $P$ , we first compute the MAT in  $P^*$ , and then answer  $\triangle e_i e_j e_k$  provide that the MAT in  $P^*$  is  $\triangle V_i^* V_j^* V_k^*$ .

A counter example is shown in Figure 17.



■ **Figure 17** The above reduction is wrong.

### C Direction $d(L_{j,k}^{HG})$ is not monotone with respect to $j$ or $k$ .

The following picture shows that  $d(L_{j,k}^{HG})$  do not has a monotonicity with respect to  $j$  or  $k$ . Similarly,  $d(L_{j,k}^{H'G'})$ ,  $d(L_{j,k}^{HG'})$ ,  $d(L_{j,k}^{H'G})$  do not has a good monotonicity either.

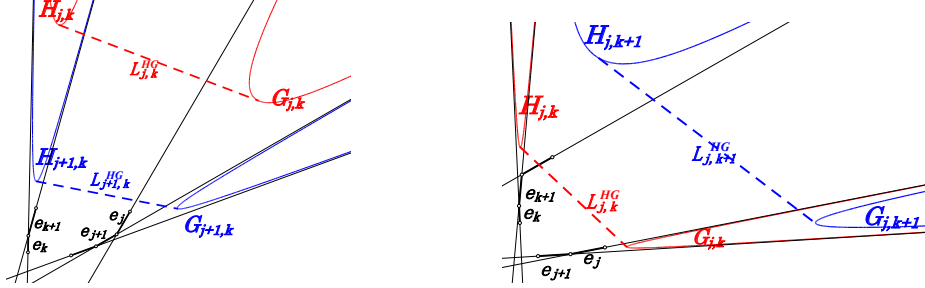


Figure 18 In the left picture,  $d(L_{j+1,k}^{HG}) < d(L_{j,k}^{HG})$ . In the right picture,  $d(L_{j,k+1}^{HG}) < d(L_{j,k}^{HG})$

### D An alternative decision-condition (without a proof)

Assume we are at iteration  $(e_j, e_k)$  now. See Figure 19. We may consider the following alternative decision-condition to kill  $j$  or kill  $k$ . Let  $e_i = \text{OPT}_{j,k}$ . If  $e_i$  lies on the right of  $L_{j,k}^{HG'}$ , kill  $j$ . Otherwise, kill  $k$ . The correctness is based on the following statements:

- (a) If  $e_i$  does not lie on the right of  $L_{j,k}^{HG'}$ , then  $(j+1, k), \dots, (j+\Delta, k)$  are dead.
- (b) If  $e_i$  lies on the right of  $L_{j,k}^{HG'}$ , then  $(j, k+1), \dots, (j, k+\Delta)$  are dead.

Statement (a) is true. It simply follows from Lemma 18. The correctness of (b) remains unknown, and is leaved as an **open problem** of this paper. If (b) is proved, we obtain another  $O(n)$  time algorithm which is slightly simpler than the one presented in Section 4.

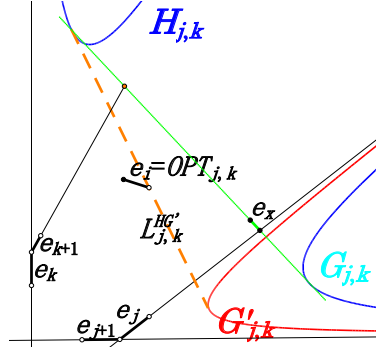


Figure 19 Illustration of another decision-condition.

**A possible approach to prove (b).** Suppose  $e_i$  lies on the right of  $L_{j,k}^{HG'}$ . We want to argue that  $(e_j, e_{k+1})$  is dead, i.e. there is no edge  $e_x$  such that  $\Delta e_j e_{k+1} e_x$  is 3-stable. Notice that there may exist  $e_x$  such that  $e_j, e_{k+1}$  are both stable - that means  $\ell_x$  intersects  $H_{j,k}$  and  $G_{j,k}$ , as shown in Figure 19. Nevertheless, we believe that  $e_x$  cannot be stable when  $\ell_x$  intersects both  $H_{j,k}$  and  $G_{j,k}$ . Specifically, we believe  $\text{Area}(\Delta e_i e_j e_{k+1}) < \text{Area}(\Delta e_x e_j e_{k+1})$ . Based on several experiments, this seems true. Therefore, (b) seems to hold.

Comparing to decision-condition presented in Section 4, the above decision-condition is more symmetric to Jin's original decision-condition for computing the MAT in [7].